doi: https://doi.org/10.5704/MOJ.2611.006

Human Umbilical Mesenchymal Stem Cell Chondrogenesis on Electrospun Fish Gelatin Scaffold

Ab-Rahim S[1], PhD, **Koh CT**[2], PhD, **Ham WJ**[2], MSc, **Alitar SR**[2], BSc, **Zulkifli NS**[2], BSc, **Muhamad M**[1], PhD

[1]Department of Biochemistry and Molecular Medicine, Universiti Teknologi MARA, Sungai Buloh, Malaysia
[2]Faculty of Mechanical and Manufacturing Engineering, Universiti Tun Hussein Onn Malaysia, Parit Raja, Malaysia



This is an open-access article distributed under the terms of the Creative Commons Attribution License, which permits unrestricted use, distribution, and reproduction in any medium, provided the original work is properly cited

Date of submission: 18th December 2024
Date of acceptance: 16th April 2026

ABSTRACT

Introduction: Articular cartilage degenerates over time owing to trauma, sports injuries and ageing. The tissue has limited repair capacity due to its avascular characteristics; hence research in articular cartilage regeneration remains challenging. A tissue engineering approach has shown promising results in restoring and regenerating injured articular cartilage tissue using biomaterials that mimic the tissue microenvironment. Thus, this study aims to investigate chondrogenic differentiation of mesenchymal stem cells (MSC) in high-density culture on a multi-layered nanofibrous scaffold towards the development of cell-based therapy for articular cartilage damage.

Materials and methods: Two types of newly developed electrospun hydrogel scaffolds were used to determine their efficacy in MSC chondrogenesis. Both scaffolds were produced from cold-water fish skin gelatine mixed with glacial acetic acid and water followed by an electrospinning technique with different rotation speeds to produce homogeneous (HS) and multilayer (MS) scaffolds. Both scaffolds were crosslinked with glutaraldehyde. Mechanical strength of the scaffolds was measured with a uniaxial test. The hUMSCs were cultured in DMEM/F-12 media with 10% foetal bovine serum. Cell cytotoxicity was measured using a cell proliferation assay on post-chondrogenesis scaffolds. Morphological assessment was performed using scanning electron microscopy. Levels of expression of chondrogenic markers, CD44, CD166, and CD151, were measured using flow cytometry after chondrogenic differentiation.

Results: Mechanical strength analysis showed that both crosslinked HS and MS presented higher tensile strength and elastic modulus compared with uncrosslinked HS and MS. Expression of the chondrogenic markers was upregulated in both scaffolds.

Conclusion: Both scaffolds promoted mesenchymal chondrogenesis, suggesting possible application for articular cartilage regeneration.

Keywords:
articular cartilage, fish skin gelatine, human umbilical stem cells, electrospun, chondrogenesis

INTRODUCTION

Osteoarthritis (OA) is a heterogeneous disease affecting senior citizens in Malaysia, for which age and obesity have been recognised as prominent risk factors as well as genetics, mechanical stress, injury, and hormonal modifications[1]. The disease is characterised by progressive damage of articular cartilage as well as bone remodelling or new bone formation (osteophytes and subchondral bone sclerosis), whereby healthy articular cartilage, which is smooth and flexible, becomes brittle and thin during disease progression[2]. The brittle cartilage offers less protection to the bones at the joints and causes excruciating pain as well as inflammation and eventually disability among OA patients, imposing a prominent economic health burden. Although the current standard treatment with glucosamine has proven effective in reducing patients' dependency on painkillers, long-term disease management is still lacking. Intervention procedures available for osteoarthritis include joint replacement, microfracture surgery, and debridement of damaged cartilage[3]. However, the result of these approaches is often non-sustainable, leading to either repeated surgery or permanent tissue damage. Another common treatment is joint replacement, usually made from a metal stem with plastic or metal components shaped similarly to the joint. As the procedure involves major surgery, post-surgery pain is

Corresponding Author: Mudiana Muhamad, Department of Biochemistry and Molecular Medicine, Faculty of Medicine, Universiti Teknologi MARA Selangor Branch, Sungai Buloh Campus, 47000 Sungai Buloh, Selangor, Malaysia
Email: mudiana_muhamad@uitm.edu.my

inescapable, with an extensive recovery period of up to two years[4]. Nonetheless, the procedure has yet to be proven a permanent solution, as 'wear and tear' of the joint replacement is inevitable over time, due to poor integration of synthetic materials with the human cells. Thus, full joint replacement is otherwise impractical for younger patients such as athletes suffering from cartilage injury.

Undoubtedly, there is a pressing need for an alternative treatment strategy that presents more sustainable long-term results. Cell-based therapy provides a promising solution, particularly using stem cells which have the capacity to differentiate into target cells. Sources of stem cells that have been studied for regeneration of various tissues include hyaline cartilage, adipocytes, bone marrow, dental pulp, amniotic fluid as well as embryos[5]. Hence, this study proposed to use a stem cell source that is less explored, human umbilical cord-derived mesenchymal stem cells (hUMSCs), a noncontroversial source compared to embryonic stem cells, and isolation from the umbilical cord instead of bone marrow provides a better non-intrusive procedure. They can differentiate into the three germ layers and promote tissue repair, modulate immune responses and exhibit anticancer properties[6]. More importantly, the chondrogenic differentiation potential of hUMSCs was thrice that of those isolated from bone marrow in producing collagen[7].

Gelatine is a popular bioactive biopolymer that is used as porous scaffolds in tissue engineering. Fish gelatine has lower amino acid contents compared to mammalian gelatines, which affects their physical and chemical characteristics[8]. In recent years, gelatine produced from cold-water fish skin[9] and salmon[10] has been considered an alternative to mammalian gelatine in tissue engineering applications. Besides having the advantageous characteristics of good biodegradability and immunogenicity, fish gelatine was used due to religious sentiments and for the reduced risk of disease outbreaks[11]. Control of microstructure morphologies is also a critical concern in the design of tissue-engineered scaffolds. One of the strategies is tuning structures to better mimic the collagen network in the extracellular matrix of native tissues[12]. The collagen network in normal cartilage was found in different fibre diameters, distribution and orientation[13]. Variations in microstructure morphologies of hydrogel scaffolds influence the mechanical environment during the osteochondral regeneration[14].

Various fabricating techniques, including freeze-drying[15,16], 3D printing[17,18] and electrospinning, were used to produce porous scaffolds in different size ranges. By using the freeze-drying method, pores were created in a range of 47±28 µm and 484±65 µm in gelatine scaffolds, which enhanced the modulus and facilitated the formation of homogeneous bovine articular chondrocytes for maintaining the chondrogenic phenotype[16]. The pore sizes were controlled by ice particles and did not exhibit an obvious effect on cell proliferation but exhibited different effects on cartilage regeneration[15]. Electrospinning is another popular technique used to produce tissue-engineered scaffolds with tuneable microstructure morphologies. Microstructure morphologies were controlled by solution concentration, gelatine bloom strength and process parameters. Fibre diameters were found to control osteoblastic cell migration and differentiation in electrospun gelatine[19].

The use of stem cells combined with biocompatible and biodegradable three-dimensional scaffolds provides a promising strategy for cell-based therapy. Therefore, this study proposed to explore the potential of a multilayer nanofibrous scaffold, which was custom-developed by our collaborators from UTHM. The scaffold comprised biomimetic nanofibres that resemble the microstructure of native cartilage. The bioactive materials component has been shown to promote excellent *de novo* integration with existing cells, and thus we hypothesised that it had ideal properties for stem cell chondrogenesis. As such, this study aims to demonstrate chondrogenic differentiation of hUMSCs induced by growth factors after high-density culture in a multi-layered nanofibrous scaffold, towards the development of a cell-based therapy 'bio-dressing' for the treatment of articular cartilage damage.

MATERIALS AND METHODS

Essentially, the study comprised the development of the scaffolds followed by their *in vitro* chondrogenesis analysis. Custom fabrication and mechanical testing of the scaffolds were performed at the Faculty of Engineering, UTHM, Johor. The subsequent *in vitro* methods were carried out in UiTM Sungai Buloh Campus, Selangor at the Institute of Molecular Medical Biotechnology (IMMB) laboratory. Essentially, the *in vitro* chondrogenesis analysis was performed on three groups, which were a homogeneous scaffold (HS), a multilayer scaffold (MS), and hUMSCs, as the control, representing mesenchymal stem cell differentiation in chondrogenesis.

In custom fabrication of scaffolds, firstly, the gelatine polymer solutions were prepared by following the previous study[20]. A 25wt% solution of cold-water fish skin gelatine with a molecular weight of 60kDa [Sigma Aldrich, USA] was mixed with 90wt% glacial acetic acid [Merck, Germany] and 10wt% water. The gelatine solution was then stirred overnight at room temperature before being loaded into a 50mL plastic syringe [Terumo, UK].

An electrospinning machine consisting of a rotating drum collector was used to produce nanofibre scaffolds. The polymer solution was loaded into a 5mL syringe with a 23g

needle for electrospinning setup. All electrospun scaffolds were produced using the same process parameters except for the rotation speed of the rotating drum. The flow rate of polymer solution was set as 0.45mL/hr. The applied voltage was controlled at 15kV and the distance between syringe tip and collector was controlled at 15cm.

Types of scaffolds studied here include a homogeneous scaffold (HS) and a multilayer scaffold (MS). Briefly, HS was electrospun with a rotating drum speed of 500 rpm, while MS was electrospun and collected consecutively using different rotation speeds of the rotating drum. Firstly, the top layer of MS was produced by rotating the drum at a speed of 3000rpm for 6 hours. The middle layer was then produced continuously by changing the rotation speed of the rotating drum to 1000rpm for 8 hours. The bottom layer was produced by rotating the drum at 500rpm for 8 hours. All scaffolds were dried in a desiccator for at least 24 hours to remove residual solvent[21].

Subsequently, the scaffolds were crosslinked with glutaraldehyde[18] [Merck, USA]. After the electrospinning process, the GTA-crosslinking process was carried out by cutting the electrospun scaffolds into rectangles and then clipping them with two rectangular fixtures. Afterwards, the scaffolds were put into a desiccator containing an aqueous GTA solution at 40˚C for 5 hours.

For analysis of scaffold morphology and strength, observation of the morphology was performed using Scanning Electron Microscopy [SEM; Hitachi SU1510, Japan] on the top view of the microstructure morphology of HS and the cross-section of MS. In order to visualise the cross-section of MS, the cross-section of the scaffolds was placed upright by sticking the scaffold to the side of a block. Each electrospun scaffold was gold-coated using a gold sputter [Fisons, UK] for 60 seconds to put a conductive surface on the polymeric electrospun scaffolds prior to SEM visualisation. The SEM images were processed using Image J software [NIH, USA] to determine fibre diameters and pore sizes. The images were captured from three random regions. Fibre diameters were measured for each image to get an average fibre diameter. The fibre pore size was determined by measuring the threshold area of the images.

Electrospun scaffolds were cut into 24 × 3mm rectangular shapes for a uniaxial tensile test using a universal testing machine [Lloyd Instruments Ltd, UK]. A 500N load cell was used for crosslinked HS and MS and stretched at a constant rate of 3.0mm/min until deformed, while a 10N load cell was used for tensile testing of uncrosslinked HS and MS. The tensile strength of, fracture strain εf, and elastic modulus E were measured from the uniaxial test. The tensile strength was the maximum stress value in the stress-strain curves. The fracture strain was the strain corresponding to the tensile strength. The elastic modulus was determined from the slope of the linear region of the stress-strain curves.

For cell culture, the human umbilical mesenchymal stem cells (hUMSC) were a kind gift from our collaborator, NiSCELL Sdn. Bhd. [Selangor, Malaysia]. The cells were cultured in a T25 flask and maintained in Dulbecco's Modified Eagle's Medium/Nutrient mixture F-12 (DMEM/F-12) supplemented with 10% foetal bovine serum (FBS) and 1% penicillin/streptomycin [Nacalai Tesque, Japan]. Once the MSCs reached 90% confluency, the cells were seeded at $1X10^5$ cells/well of the 2 types of scaffold plates (6-well plate): the homogeneous and the multilayer electrospun scaffolds. The cultured cells were maintained at 37°C in a humidified incubator with the presence of CO_2 at 5% and regularly observed using an inverted microscope [Olympus, Japan]. The medium was changed every 2 days. The final observation was taken on day 4 before testing for cell viability using a cell proliferation assay.

In the in vitro chondrogenesis analysis, the SEM of the cells on scaffolds involved human umbilical mesenchymal stem cells (hUMSC) that were seeded on the scaffold at a cell density of 1.0×10^5/well and cultured for 4 days. Cells were fixed with 2.5% glutaraldehyde for 30 minutes, followed by post-fixation with 1.0% osmium oxide for 1 hour. Samples were dehydrated gradually in ethanol with 30, 50, 60, 70, 80, and 90% concentrations, respectively, at 4°C for 5 minutes. For dehydration with 100% ethanol, the process was done at room temperature instead of at 4°C. Subsequently, the samples were further dried using a chemical drying method. Samples were dried with an ethanol and hexamethyldisilazane (HMDS) mixture at the ratio of 1:1, 1:3 and 100% HMDS for 10 minutes for each concentration and under a fume hood. Samples were coated with a conductive element using a sputter coater before being observed under a benchtop SEM [Hitachi TM3000].

The MSC viability on both types of scaffolds was measured using a CellTiter 96 AQueous One Solution assay kit according to the manufacturer's protocol [Promega, USA] with minor modifications. The seeded cells were cultured for 2 and 4 days on the scaffold prior to the assay. Briefly, 200 µl of MTS reagent was added to each well, including the control. The plate was incubated at 37°C in a humidified incubator with the presence of CO_2 at 5% for 2 hours. After 2 hours, the medium of each well was transferred into a 96-well plate, respectively, and read at an absorbance of 490nm. Viability Calculation = [(Mean of Scaffolding - mean Blank) / (Mean of control – mean blank)] x 100.

The human umbilical cord mesenchymal stem cells (hUMSCs) were cultured and expanded in a T-25 flask with growth media consisting of DMEM F/12, 10% FBS, and 1% penicillin/streptomycin. The cells were then incubated at 37°C with 5% CO_2 until they reached approximately 80% confluency. Upon reaching this stage, the cells were detached from the flask and centrifuged at 1500 rpm for 5 minutes.

Approximately 3×10^5 cells were then seeded into a 6-well plate containing MLS and HS scaffolds. The cells were incubated at 37°C with 5% CO_2 for 2 hours to allow for proper adhesion to the scaffolds. Afterward, 0.2mL of chondrogenic medium, composed of 1X StemPro® Osteocyte/Chondrocyte Differentiation Basal Medium and 1X StemPro® Chondrogenesis Supplement (Gibco), was gently added to each well. This medium was further supplemented with 50µg/mL ascorbic acid, 40µg/mL proline, 1% insulin-transferrin-selenium (ITS+1), 0.1µmol/L dexamethasone [all from Sigma-Aldrich, USA], and 10ng/mL IGF-1 growth factor [R&D Systems, USA]. The cells were cultured under the same conditions for 21 days, with the medium being exchanged every 3 to 4 days to ensure proper nutrient supply and growth conditions. The expression of chondrogenic markers was measured with flow cytometry. Briefly, hUMSCs cultured on both scaffolds were trypsinised and resuspended in staining buffer consisting of 5% FBS and 1X PBS at a final concentration of 1x106 cells/mL for every sample. Four 12x75mm round-bottom tubes were labelled and 100µl of the hUMSCs cell suspension was aliquoted to each of the tubes. About 5µl of each monoclonal antibody marker, CD44, CD166, CD151, CD34, CD90, and CD73, was added to the round-bottom tubes, and the tubes were pulse-vortexed to mix. The samples were incubated on ice for 1 hour in the dark and protected from light. The cells were washed with cold staining buffer and centrifuged at 1500 rpm for 5 min at room temperature. Next, the cells were resuspended in the staining buffer and analysed by using BD FACS CytoFLEX S.

Statistical analysis of the biochemical analysis was executed using the Statistical Package for the Social Sciences (SPSS). The experiments were carried out three times and in triplicate for each experiment. All sets of data were checked for their normal distribution and then analysed using one-way ANOVA for comparison between more than two groups with Tukey's post hoc test. Data were expressed as mean ± SEM. Statistical significance was defined as $p<0.05$.

RESULTS

The scanning electron microscopy (SEM) images in Fig. 1 presented the top view of homogeneous scaffold (HS) and the side view of the multilayer scaffold (MS). The top view of HS (Fig. 1a) showed the morphology of fibre networks without bead formation, with a pore size of 502 ± 17nm and a fibre diameter of 824 ± 85nm. While HS was expected to have a homogeneous structure throughout the cross-sectional area, MS was observed to have microstructure gradient structures over its thickness. The top layer of MS is supposed to have a similar microstructure to the HS. The SEM images of the side view of MS (Fig. 1b) showed three different layers with changes in microstructural architecture over the sample thickness. The pore sizes of the MS increase as the gradient changes from top to bottom layer.

Fig. 2 represents the mechanical analysis of uncrosslinked and crosslinked HS and MS. In comparison to uncrosslinked scaffolds, the crosslinked HS and MS possessed higher tensile strength and elastic modulus. The elastic modulus of crosslinked HS (E = 387.85 ± 55.99 MPa) was larger than that of the crosslinked MS (E = 248.82 ± 173.34 MPa) (Fig. 2b). However, fracture properties including tensile strength and fracture strain were quite similar in both crosslinked scaffolds.

The contact angle was measured to evaluate the hydrophilicity of the scaffolds, as shown in Fig. 3. The contact angle of MS was quite similar to that of HS with both scaffolds having high hydrophilicity. The time history of the contact angle showed a decreasing trend in contact angle measurement after 5 seconds and 10 seconds, demonstrating that the electrospun scaffolds absorb and are thus suitable for cell adhesion and growth.

Assessment of hUMSC morphology on both types of scaffolds using phase contrast microscopy on day 2 post-chondrogenesis showed that fibroblast-shaped cells proliferated extensively with the cell growth orientation parallel to each other in one direction (Fig. 4a and b). However, on day 4, it was observed that the cells stopped proliferating and produced more gaps in both scaffolds (Fig. 4c and 4d). The orientation of the cells was also changed to random directions. Interestingly, on day 4 MS was observed to create folding lines, which were not seen in HS.

SEM analysis showed cells scattered and spheroidal in shape, which gradually condensed as clusters and existed as hybrids in both types of scaffolds. The secreted ECM was observed as a network secreted and accumulated surrounding the cells on the surface of both scaffolds. The morphology of the cells was apparent, with projections of appendices from clustered cells, as shown in Fig. 5. The SEM showed cell-cell interaction by extending filopodia from the edges of cells towards the nearby cells. The establishment of cell-cell junctions can be seen in between the cells. Besides, some of the filopodia tips were spiked to the electrospun scaffolds, showing the interaction in between the cells and fibres.

The viability of hUMSC cultured on both scaffolds was above 80%, which indicates low to no cytotoxicity to the cells as presented in Fig. 6. However, viability of hUMSC cultured on HS was shown to be significantly higher (97.9%) than that of those cultured on MS (82.5%). The viability of the cells cultured on the HS was also shown to be comparable (97.9%) to the control (without scaffold) group. Flow cytometry analysis results presented in Table I showed that hUMSCs were positive for two of the MSC markers, which are CD90 and CD73 at 21 days post-induction of

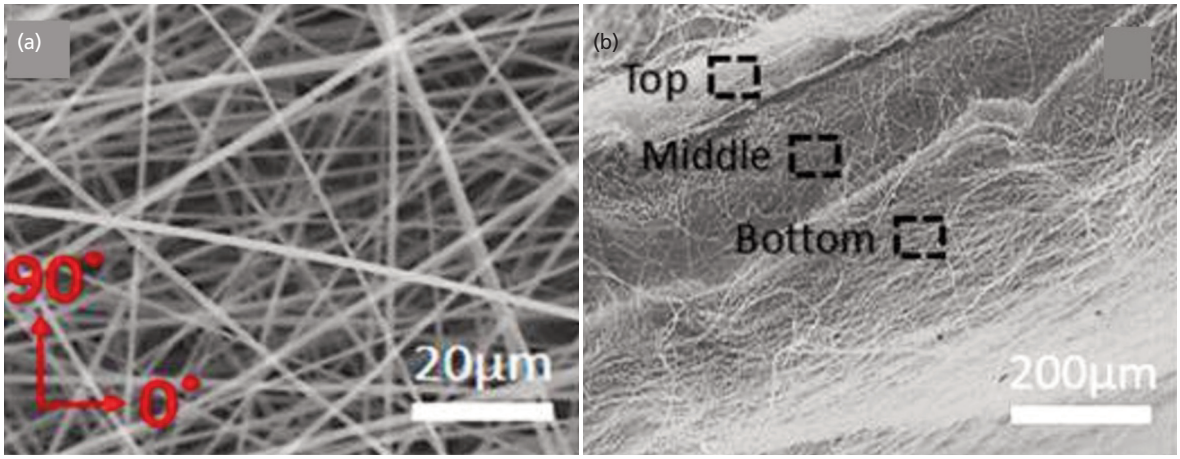

Fig. 1: Scanning electron microscopy (SEM) micrograph of (a) the top view of the homogeneous scaffold (HS) and (b) the side view of the multilayer scaffold (MS).

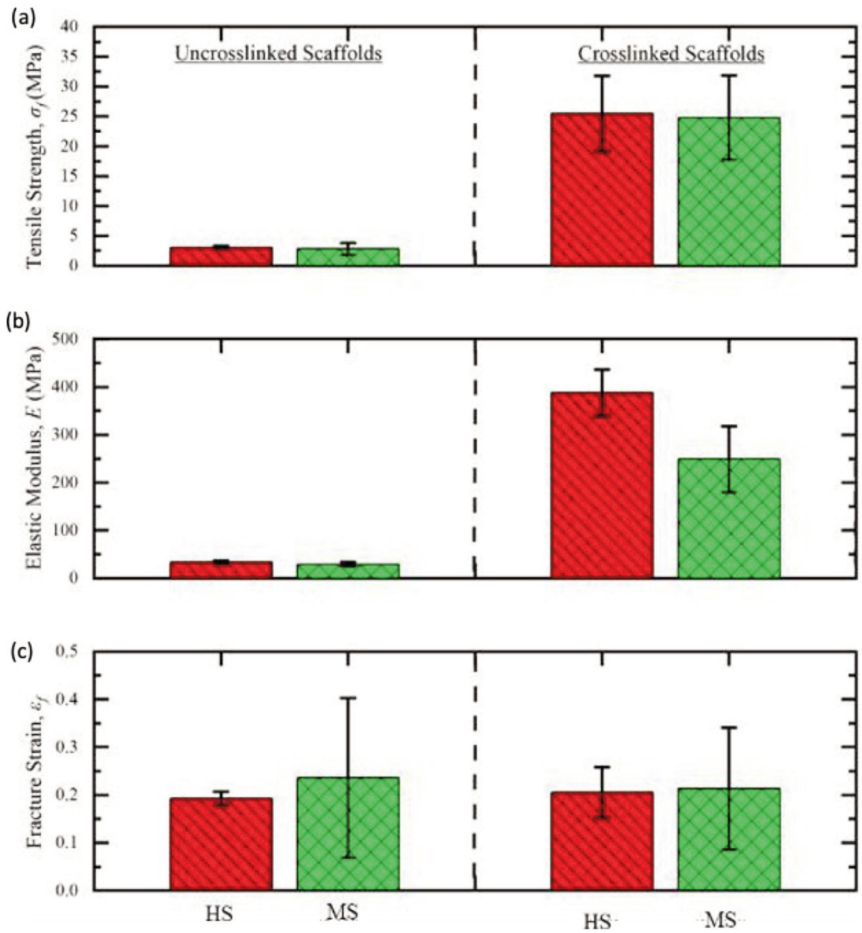

Fig. 2: The mechanical analysis of uncrosslinked and crosslinked homogeneous scaffold (HS) presented in 'red' bar and multilayered scaffold (MS) presented in 'green' bar on (a) tensile strength, (b) elastic modulus and (c) fracture strain.

chondrogenesis. However, no expression was observed for CD105 in both scaffolds, indicating that differentiation of the hUMSCs had taken place (Fig. 7). On the other hand, chondrogenic markers show high levels of expression of cell condensation markers: CD44 (hyaluronan receptor), CD166 (ALCAM), and CD151 (tetraspanins), indicating chondrogenic potential of the stem cell population (Fig. 8).

DISCUSSION

In tissue engineering, different degrees of alignment and microstructure of nanofibers affect the physiological and mechanical properties. The ability to imitate these anisotropic qualities is critical in tissue engineering because they control cell adhesion, differentiation, and proliferation[22].

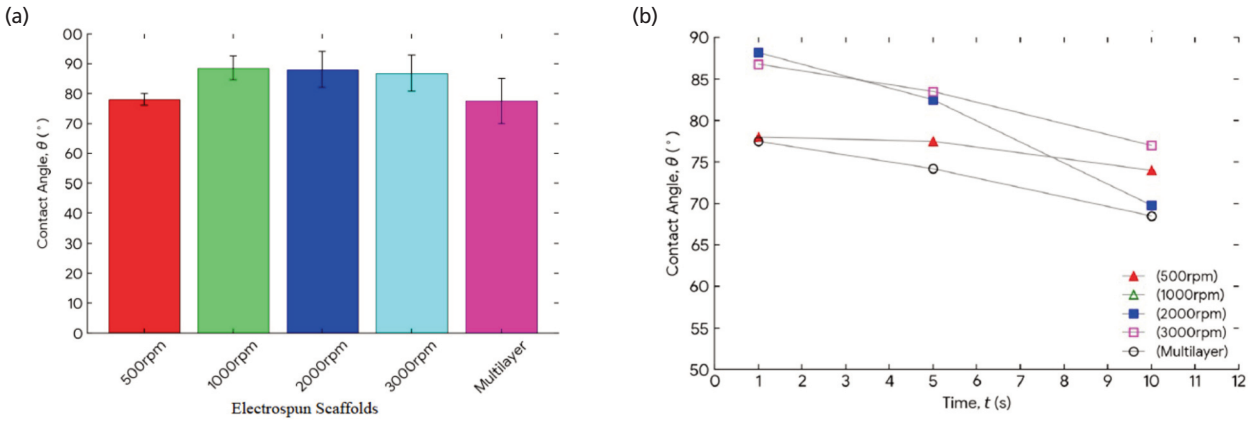

Fig. 3: Contact angle of the homogeneous scaffold (HS) and multilayer scaffold (MS) in (a) at the first second and (b) time history.

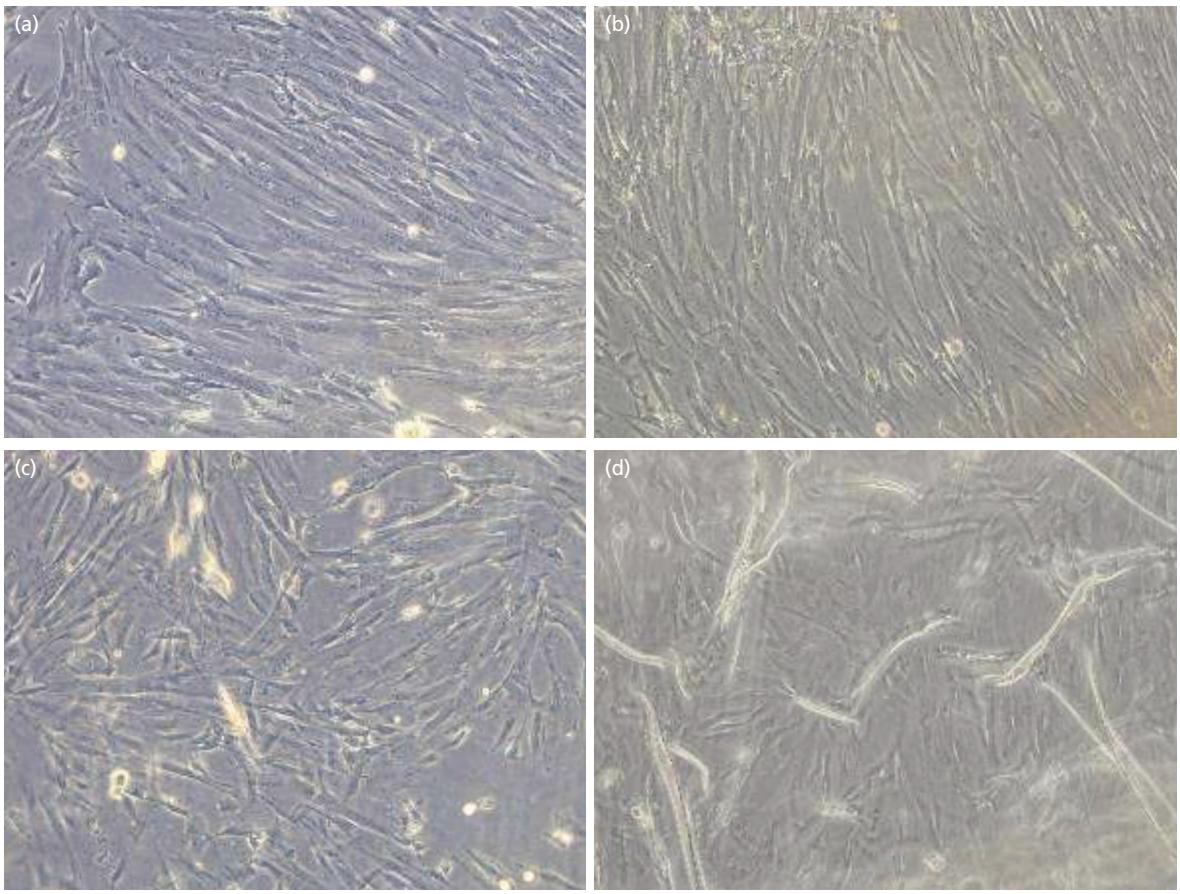

Fig. 4: Microscopic examination of hUMSC morphology on multilayer scaffold (MS) (a and b) and homogeneous scaffold (HS), (c and d) on day 2 and 4, respectively before induction of chondrogenesis. Images were captured under 100x magnification.

The multilayer scaffold (MS) featuring a gradient in degrees of fibre alignment across its thickness was fabricated using a sequential electrospinning method. The fibre alignment and density were reduced across the scaffold thickness by reducing the rotating speed of the collector drum from 3000 rpm to 1000 rpm and then to 500 rpm. However, the chemical composition of the scaffolds was maintained throughout the fabrication process.

While studies suggest that the fibre alignment influences the mechanical properties[20,23], the MS is expected to have a gradient in mechanical properties across its thickness. The mechanical testing result (Fig. 2) shows that the Young's modulus of MS was smaller than that of homogeneous scaffold (HS). The MS presented similar fracture properties in both fracture strain and strength as compared to that of HS.

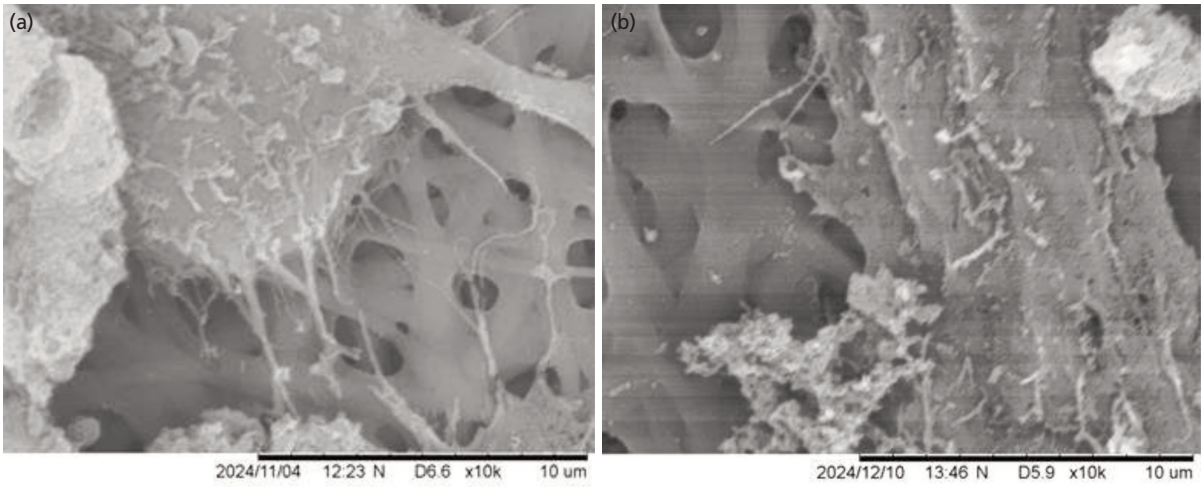

Fig. 5: Scanning electron microscopy (SEM) micrograph of hUMSC on the surface of (a) homogeneous scaffold (HS) and (b) multilayered scaffold (MS) at magnification x10000.

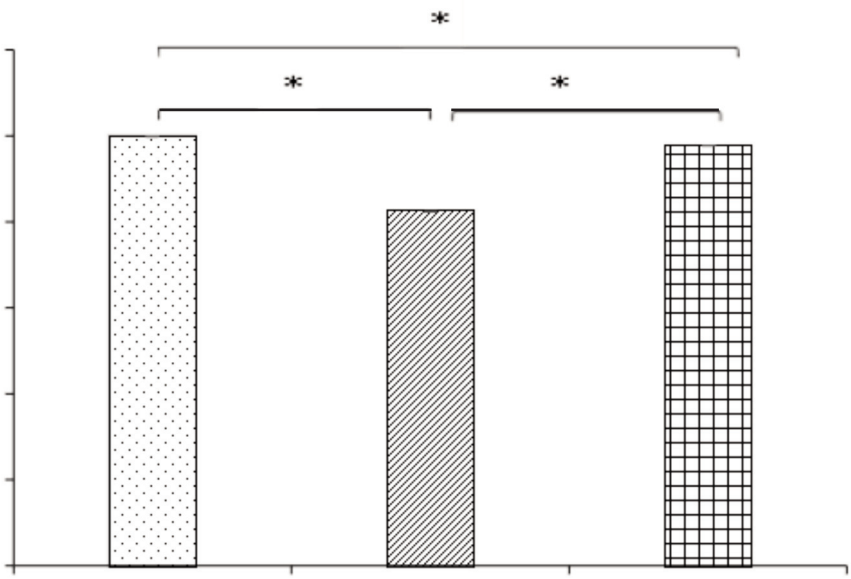

ç		MS	HS
OD (MEAN±SDEV)	2.231±0.04	1.878±0.03	2.190±0.05
VIABILITY (%)	100%	82.50%	97.90%

*Denotes significant level at P<0.05

Fig. 6: Viability of hUMSC cultured on multilayer scaffold (MS) and homogeneous scaffold (HS). The experiments were conducted 3 times (N=3) with triplicates for each experiment.

Microscopic observation showed hUMSCs grown on both scaffolds were comparable to the control, whereby the cells were confluent by day 2 of culture. On day 4, it was observed that both scaffolds were packed with cells; however, structure loss was observed in HS, as seen by the folding lines of the scaffolds. The bigger pore size in HS increases the deposition of extracellular matrix (ECM), which further loosens the fibre arrangement of the scaffold; thus, the folding lines were observed. This finding is further supported by the scanning electron microscopy (SEM) results, whereby numerous cells form aggregates on the HS, with ECM deposition surrounding the cell aggregates at day 14 post-chondrogenesis induction. On the other hand, the microstructure of MS was maintained, which could be due to

Table I: The expression of MSC and chondrogenic markers of the hUMSC at 21 days post-induction on the multilayered (MLS) and homogeneous (HS) scaffolds, expressed as the mean (% cells).

Markers	Antibody	Scaffold	Mean (% of cells)
MSC	CD73	Control	99.7
		Multilayered Scaffold	97.8
		Homogeneous Scaffold	98.2
	CD90	Control	99.6
		Multilayered Scaffold	97.7
		Homogeneous Scaffold	98.2
	CD105	Control	0.5
		Multilayered Scaffold	0.2
		Homogeneous Scaffold	0.3
Chondrogenic potential	CD44	Control	98.5
		Multilayered Scaffold	96
		Homogeneous Scaffold	97.4
	CD166	Control	97.8
		Multilayered Scaffold	93.8
		Homogeneous Scaffold	95.9
	CD151	Control	98.5
		Multilayered Scaffold	94.1
		Homogeneous Scaffold	96.1

the gradient fibre formation whereby the second and third layers had bigger pore sizes, thus providing more space for cell proliferation. In addition, MS has a smaller Young's modulus, hence more flexibility compared to HS. Nonetheless, HS exhibited higher cell viability compared to MS. A previous study reported an increase of 50% in cell density along with pore size and porosity attributable to increased mass transport of nutrients and gases to the cells. However, the synthesis of cartilaginous matrix proteins significantly decreased by 40% with the pore size[24].

The expression of stem cell positive biomarkers, CD73 and CD90, was shown to be significantly high on both MS and HS with 97.8% and 98.2%, respectively, which is comparable with the control group (99.7%). The increase in CD73 is an indicator of increased plasticity of the mesenchymal stem cells (MSCs)[25], as found in this study with hUMSCs, which in turn enhances their differentiation potential into osteogenic and chondrogenic lineages *in vitro*. Moreover, the relatively comparable expression with the control indicated similar superior differentiation capacity of both scaffolds. Interestingly, the expression of CD90 remains significantly high in the hUMSCs after differentiation. Our finding is in line with a previous study that reported consistent CD90 expression after osteogenic differentiation of MSCs[26]. A previous study also showed that CD90+ increased the chondrogenic potential of synovial fluid mesenchymal progenitor cells[27]. However, CD90 was also shown to be highly expressed in fibrocartilage tissues[28].

On the other hand, CD105 was not expressed in all 3 groups, even though the chondrogenic potential of MSCs is often linked to CD105 expression[29], which is contradictory to this study's findings. However, a previous study has reported a subpopulation of MSCs that is negative for CD105. In addition, Cleary *et al* (2016) showed that expression of CD105 on expanded bone marrow MSCs does not predict their chondrogenic potential, while Varma *et al* (2007) also reported a low level of CD105 in freshly isolated MSCs from adipose tissue[30,31]. Since the data on CD105+ expression vary depending on the source of the stem cells, the finding from this study could imply that CD105 may not be a useful marker for *in vitro* MSC detection, as suggested by Lin *et al* (2013)[32]. Nevertheless, chondrogenic potential markers, CD44, CD166, and CD151 were highly expressed in the hUMSC culture on both scaffolds.

Hydrogel scaffolds that actively support chondrogenesis, such as those used in this study, are transformative for cartilage repair because they address the critical limitation of cell "dedifferentiation" (loss of function) commonly seen in traditional therapies. By mimicking the physicochemical properties of the native extracellular matrix (ECM), these scaffolds maintain the spherical phenotype of encapsulated chondrocytes while guiding the MSCs toward cartilage lineage rather than fibrous tissue. This bio-instructive capability translates into versatile clinical applications. Foremost is minimally invasive therapy, where injectable hydrogels can recover irregular osteochondral defects and polymerise in situ, ensuring seamless integration with host tissue without open surgery. Moreover, these scaffolds present sophisticated delivery systems, allowing controlled release of chondrogenic factors (like TGF-β) or anti-inflammatory agents and hence halting osteoarthritis progression. In advanced scenarios, 3D bioprinting utilises these hydrogels as "bio-inks" towards fabrication of patient-specific implants that match the precise anatomical curvature of a joint. Ultimately, by providing a conducive 3D microenvironment, these scaffolds shift the outcome from forming inferior scar tissue (fibrocartilage) to regenerating functional, load-bearing hyaline cartilage.

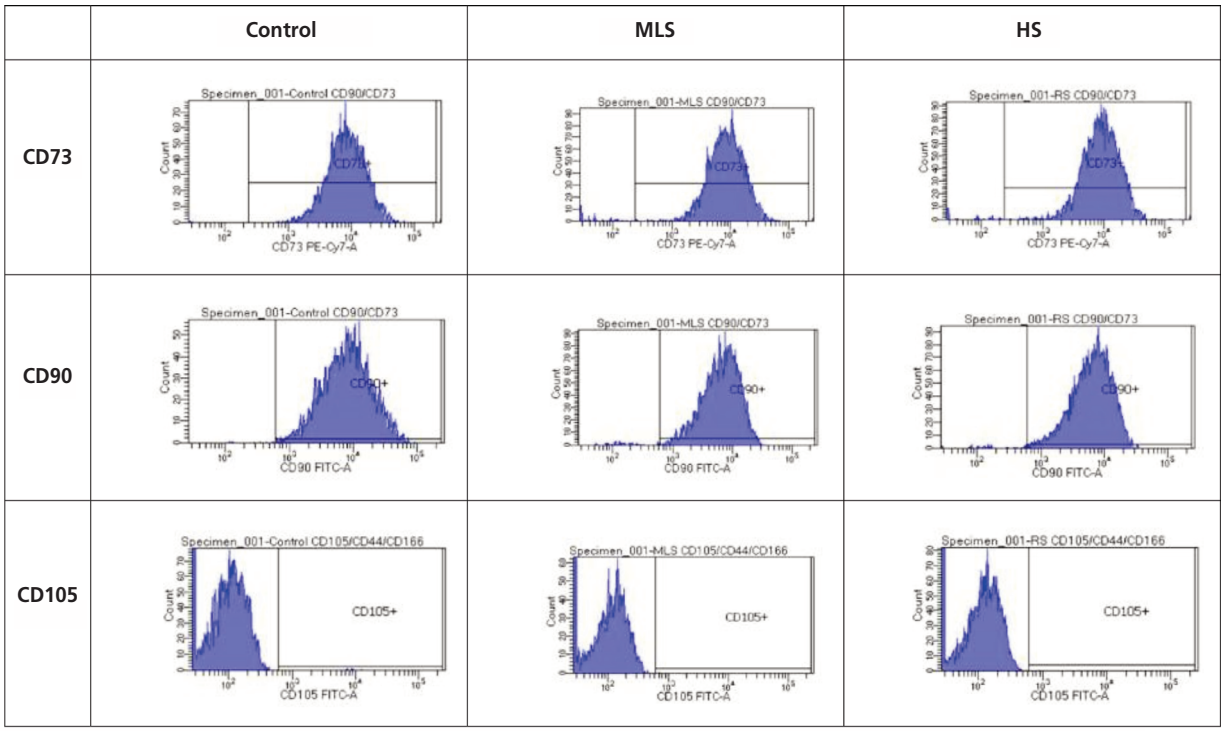

Fig. 7: Histograms of the level of expression of mesenchymal stem cells (MSCs) positive CD markers.

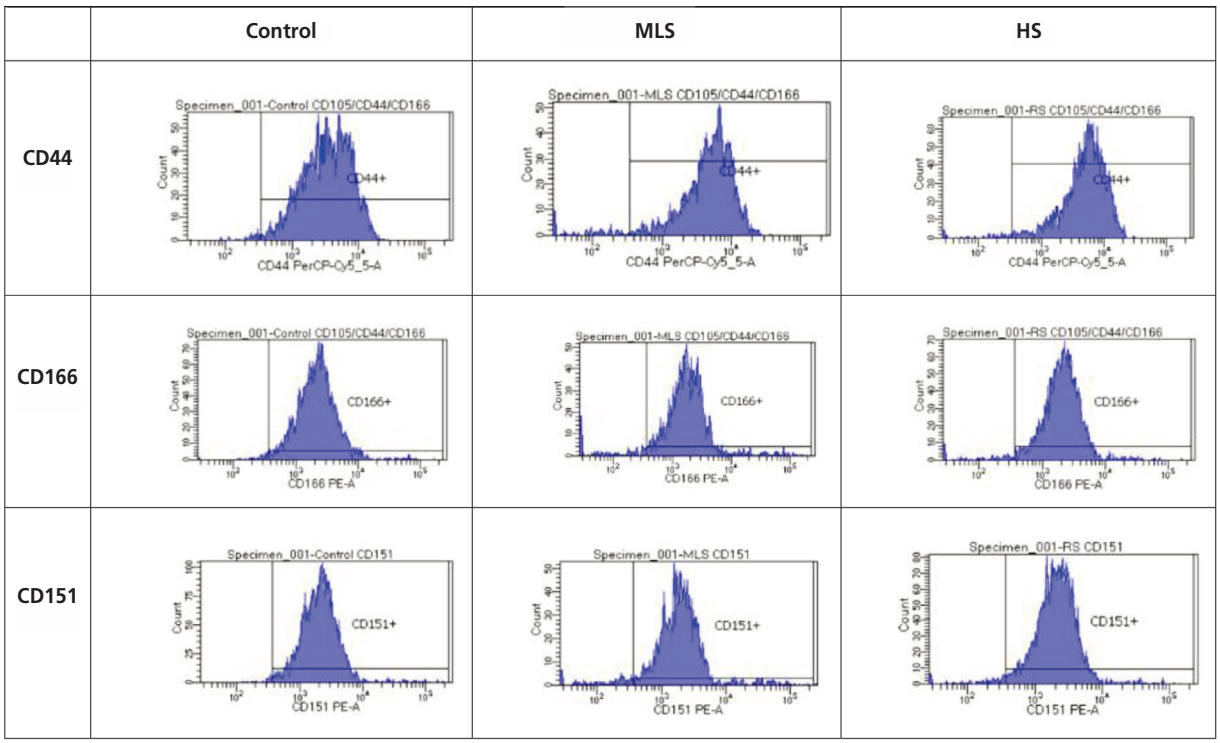

Fig. 8: Histograms of the level of expression of chondrogenesis potential markers.

Despite the positive findings in this study, the scaffolds present several drawbacks. These materials' mechanical strength and wear resistance to endure the significant compressive and shear forces within joints with the cells incorporated were not tested. Moreover, *in vivo* studies using animal models need to be carried out to elucidate cell infiltration, nutrient diffusion within the scaffolds, and adhesion to subchondral bone and surrounding tissues. Manufacturing inconsistencies, sterilisation difficulties, and potential inflammatory reactions also pose challenges to clinical application and long-term effectiveness in demanding orthopaedic procedures currently.

CONCLUSION

Based on the results, although the percentage of MSC marker expression was high, the scaffold still potentially provides the cell environment and microstructure for hUMSCs to differentiate into chondrocytes. These findings evidently showed the potential of both scaffolds in promoting chondrogenesis of hUMSC. Nevertheless, further analysis is necessary for the determination of phenotypic consistency of the differentiated hUMSC.

ACKNOWLEDGEMENT

The authors acknowledge Universiti Tun Hussein Onn Malaysia (UTHM)[GPPS/H715] for the research grant provision for this study, as well as the Centre of Graduate Studies (CGS) of UTHM. The authors also wish to acknowledge Ms. Izzah Munirah Hanapi for the completion of SEM work.

CONFLICT OF INTEREST

The authors declare no conflict of interest.

REFERENCES

1. Foo CN, Arumugam M, Rampal L, Lye MS, Mohd-Sidik S, Jamil-Osman Z. Knee pain and functional disability of knee osteoarthritis patients seen at Malaysian government hospitals. *Malays J Med Health Sci.* 2017; 13(2): 7-15.
2. Zhu X, Chan YT, Yung PSH, Tuan RS, Jiang Y. Subchondral Bone Remodeling: A Therapeutic Target for Osteoarthritis. *Front Cell Dev Biol.* 2021; 8: 607764. doi: 10.3389/fcell.2020.607764
3. Tay LX, Ahmad RE, Dashtdar H, Tay KW, Masjuddin T, Ab-Rahim S, *et al.* Treatment outcomes of alginate-embedded allogenic mesenchymal stem cells versus autologous chondrocytes for the repair of focal articular cartilage defects in a rabbit model. *Am J Sports Med.* 2012; 40(1): 83-90. doi: 10.1177/0363546511420819
4. Greene A, Miles C. Surgery avoidance rates among total knee replacement candidates following a non-invasive biomechanical intervention: A retrospective cohort study. *J Orthop Exp Innov.* 2022; 3(2). doi: 10.60118/001c.37664
5. Zuliani CC, Damas II, Andrade KC, Westin CB, Moraes ÂM, Coimbra IB. Chondrogenesis of human amniotic fluid stem cells in Chitosan-Xanthan scaffold for cartilage tissue engineering. *Sci Rep.* 2021; 11(1): 3063. doi: 10.1038/s41598-021-82341-x
6. De Miguel MP, Fuentes-Julián S, Blázquez-Martínez A, Pascual CY, Aller MA, Arias J, Arnalich-Montiel F. Immunosuppressive properties of mesenchymal stem cells: advances and applications. *Curr Mol Med.* 2012; 12(5): 574-91. doi: 10.2174/156652412800619950
7. Fong CY, Subramanian A, Gauthaman K, Venugopal J, Biswas A, Ramakrishna S, Bongso A. Human umbilical cord Wharton's jelly stem cells undergo enhanced chondrogenic differentiation when grown on nanofibrous scaffolds and in a sequential two-stage culture medium environment. *Stem Cell Rev Rep.* 2012; 8(1): 195-209. doi: 10.1007/s12015-011-9289-8
8. Gómez-Guillén MC, Pérez-Mateos M, Gómez-Estaca J, López-Caballero E, Giménez B, Montero P. Fish gelatin: a renewable material for developing active biodegradable films. *Trends Food Sci Technol.* 2009; 20(1): 3-16. doi: 10.1016/j.tifs.2008.10.002
9. Yoon HJ, Shin SR, Cha JM, Lee SH, Kim JH, Do JT, Song H, Bae H. Cold Water Fish Gelatin Methacryloyl Hydrogel for Tissue Engineering Application. *PLoS One.* 2016; 11(10): e0163902. doi: 10.1371/journal.pone.0163902

10. Acevedo CA, Sánchez E, Orellana N, Morales P, Olguín Y, Brown DI, *et al.* Re-Epithelialization Appraisal of Skin Wound in a Porcine Model Using a Salmon-Gelatin Based Biomaterial as Wound Dressing. *Pharmaceutics.* 2019; 11(5): 196. doi: 10.3390/pharmaceutics11050196
11. Karim AA, Bhat R. Fish gelatin: properties, challenges, and prospects as an alternative to mammalian gelatins. *Food Hydrocoll.* 2009; 23(3): 563-76. doi: 10.1016/j.foodhyd.2008.07.002
12. Li X, Sun Q, Li Q, Kawazoe N, Chen G. Functional Hydrogels With Tunable Structures and Properties for Tissue Engineering Applications. *Front Chem.* 2018; 6: 499. doi: 10.3389/fchem.2018.00499
13. Changoor A, Nelea M, Méthot S, Tran-Khanh N, Chevrier A, Restrepo A, *et al.* Structural characteristics of the collagen network in human normal, degraded and repair articular cartilages observed in polarized light and scanning electron microscopies. *Osteoarthr Cartil.* 2011; 19(12): 1458-68. doi: 10.1016/j.joca.2011.09.007
14. Davis S, Roldo M, Blunn G, Tozzi G, Roncada T. Influence of the Mechanical Environment on the Regeneration of Osteochondral Defects. *Front Bioeng Biotechnol.* 2021; 9: 603408. doi: 10.3389/fbioe.2021.603408
15. Zhang Q, Lu H, Kawazoe N, Chen G. Pore size effect of collagen scaffolds on cartilage regeneration. *Acta Biomater.* 2014; 10(5): 2005-13. doi: 10.1016/j.actbio.2013.12.042
16. Chen S, Zhang Q, Nakamoto T, Kawazoe N, Chen G. Gelatin Scaffolds with Controlled Pore Structure and Mechanical Property for Cartilage Tissue Engineering. *Tissue Eng Part C Methods.* 2016; 22(3): 189-98. doi: 10.1089/ten.TEC.2015.0281
17. Liu J, Li L, Suo H, Yan M, Yin J, Fu J. 3D printing of biomimetic multi-layered GelMA/nHA scaffold for osteochondral defect repair. *Mater Des.* 2019; 171: 107708. doi: 10.1016/j.matdes.2019.107708
18. Li Q, Xu S, Feng Q, Dai Q, Yao L, Zhang Y, *et al.* 3D printed silk-gelatin hydrogel scaffold with different porous structure and cell seeding strategy for cartilage regeneration. *Bioact Mater.* 2021; 6(10): 3396-410. doi: 10.1016/j.bioactmat.2021.03.013
19. Sisson K, Zhang C, Farach−Carson MC, Chase DB, Rabolt JF. Fiber diameters control osteoblastic cell migration and differentiation in electrospun gelatin. *J Biomed Mater Res.* 2010; 94(4): 1312-20. doi: 10.1002/jbm.a.32756
20. Khoo W, Chung SM, Lim SC, Low CY, Shapiro JM, Koh CT. Fracture behavior of multilayer fibrous scaffolds featuring microstructural gradients. *Mater Des.* 2019; 184: 108184.
21. Ham WJ, Koh CT. Electrospinning of aligned nanofibers for biomedical application using a rotating drum collector. *Malays J Microsc.* 2021; 17(2).
22. Mitchell GR, Tojeira A. Role of anisotropy in tissue engineering. *Proc Eng.* 2013; 59: 117-25.
23. Nivison-Smith L, Weiss AS. Alignment of human vascular smooth muscle cells on parallel electrospun synthetic elastin fibers. *J Biomed Mater Res A.* 2012; 100(1): 155-61. doi: 10.1002/jbm.a.33255
24. Nava MM, Draghi L, Giordano C, Pietrabissa R. The effect of scaffold pore size in cartilage tissue engineering. *J Appl Biomater Funct Mater.* 2016; 14(3): e223-9. doi: 10.5301/jabfm.5000302
25. Kimura K, Breitbach M, Schildberg FA, Hesse M, Fleischmann BK. Bone marrow CD73+ mesenchymal stem cells display increased stemness in vitro and promote fracture healing *in vivo. Bone Rep.* 2021; 15: 101133. doi: 10.1016/j.bonr.2021.101133
26. Cao Y, Boss AL, Bolam SM, Munro JT, Crawford H, Dalbeth N, *et al.* In Vitro Cell Surface Marker Expression on Mesenchymal Stem Cell Cultures does not Reflect Their Ex Vivo Phenotype. *Stem Cell Rev Rep.* 2024; 20(6): 1656-66. doi: 10.1007/s12015-024-10743-1
27. Krawetz RJ, Wu YE, Martin L, Rattner JB, Matyas JR, Hart DA. Synovial fluid progenitors expressing CD90+ from normal but not osteoarthritic joints undergo chondrogenic differentiation without micro-mass culture. *PLoS One.* 2012; 7(8): e43616. doi: 10.1371/journal.pone.0043616
28. Wang Y, Li Q, Li H, Yang X, Fang H, Bi R, *et al.* Heterogeneous Characteristics of the CD90+ Progenitors in the Fibrocartilage of Different Joints. *Cartilage.* 2025; 16(2): 190-201. doi: 10.1177/19476035231200359
29. Fan W, Li J, Wang Y, Pan J, Li S, Zhu L, *et al.* CD105 promotes chondrogenesis of synovium-derived mesenchymal stem cells through Smad2 signaling. *Biochem Biophys Res Commun.* 2016; 474(2): 338-44. doi: 10.1016/j.bbrc.2016.04.101

30. Cleary MA, Narcisi R, Focke K, van der Linden R, Brama PA, van Osch GJ. Expression of CD105 on expanded mesenchymal stem cells does not predict their chondrogenic potential. *Osteoarthritis Cartilage.* 2016; 24(5): 868-72. doi: 10.1016/j.joca.2015.11.018
31. Varma MJO, Breuls RGM, Schouten TE, Jurgens WJFM, Bontkes HJ, Schuurhuis GJ, *et al.* Phenotypical and functional characterization of freshly isolated adipose tissue-derived stem cells. *Stem Cells Dev.* 2007; 16(1): 91-104. doi: 10.1089/scd.2006.0026
32. Lin CS, Xin ZC, Dai J, Lue TF. Commonly used mesenchymal stem cell markers and tracking labels: Limitations and challenges. *Histol Histopathol.* 2013; 28(9): 1109-16. doi: 10.14670/HH-28.1109

Cite this article:

Ab-Rahim S, Koh CT, Ham WJ, Alitar SR, Zulkifli NS, Muhamad M. Human Umbilical Mesenchymal Stem Cell Chondrogenesis on Electrospun Fish Gelatin Scaffold. *Malays Orthop J.* 2026; 20(3): 47-58. doi: 10.5704/MOJ.2611.006